

Supporting information

Leaf Vein-Inspired Hierarchical Wedge-Shaped Tracks on Flexible Substrate for Enhanced Directional Water Collection

Jianbin Lin, Xianhua Tan, Tielin Shi, Zirong Tang, Guanglan Liao*

Huazhong University of Science & Technology, Wuhan 430074, China

* Email: guanglan.liao@hust.edu.cn

Table S1. The detailed dimensions of the tracks prepared in this work. All wedge angles of individual tracks are 1 °, and the minimum dimension of the top side of track is 0.03 mm.

		1Ls	2Ls	3Ls	4Ls
1-L	D_1	0.03 mm	0.040 mm	0.60 mm	0.55 mm
	L_1	50 mm	50 mm	50 mm	50 mm
	α	1 °	1 °	1 °	1 °
	T_1	0.94 mm	1.30 mm	—	—
2- L	D_2	—	0.03 mm	0.30 mm	0.30 mm
	L_2	—	0.66 mm	28.49 mm	28.50 mm
	α	—	1 °	1 °	1 °
	ϕ_{12}	—	60 °	60 °	60 °
	T_2	—	0.10 mm	5.22 mm	5.30 mm
3- L	D_3	—	—	0.03 mm	0.07 mm
	L_3	—	—	4.74 mm	4.87 mm
	α	—	—	1 °	1 °
	ϕ_{23}	—	—	60 °	60 °
	T_3	—	—	0.17 mm	1.86 mm
4- L	D_4	—	—	—	0.03 mm
	L_4	—	—	—	0.96 mm
	α	—	—	—	1 °
	ϕ_{34}	—	—	—	60 °
	T_4	—	—	—	0.11 mm

Table S2. Performance in this work compared with previous works.

	Structure type	Humidity	Distance (cm)	Temperature (°C)	Flow rate (m s ⁻¹)	Size (cm×cm)	Efficiency (mg cm ⁻² h ⁻¹)
Our work	Track inspired by leaf-vein	0.35 L h ⁻¹	10	6±0.5	0.6	5×5	467.30
		60-70 %	100	6±0.5	0	5×5	18.22
Ref. 30	Hierarchical microcone	336 L h ⁻¹	-	25	2	15×5	21
Ref. 31	Line track	90-95 %	-	22	-	2.5×2.5	30
Ref. 36	wettability-patterning	80 %	-	2.3±0.5	-	10×6.5	0.15
Ref. 57	Graphene on Cu foil	80-85 %	-	7±0.1	-	1×3	61.6
Ref. 58	Mesh on copper	-	8	20	0.1	4×5	200
Ref. 63	Mesh	fog+rain	-	-	dynamic	4500×2000	250
Ref. 64	Mesh	air	-	-	2.3	1000×1000	3.5

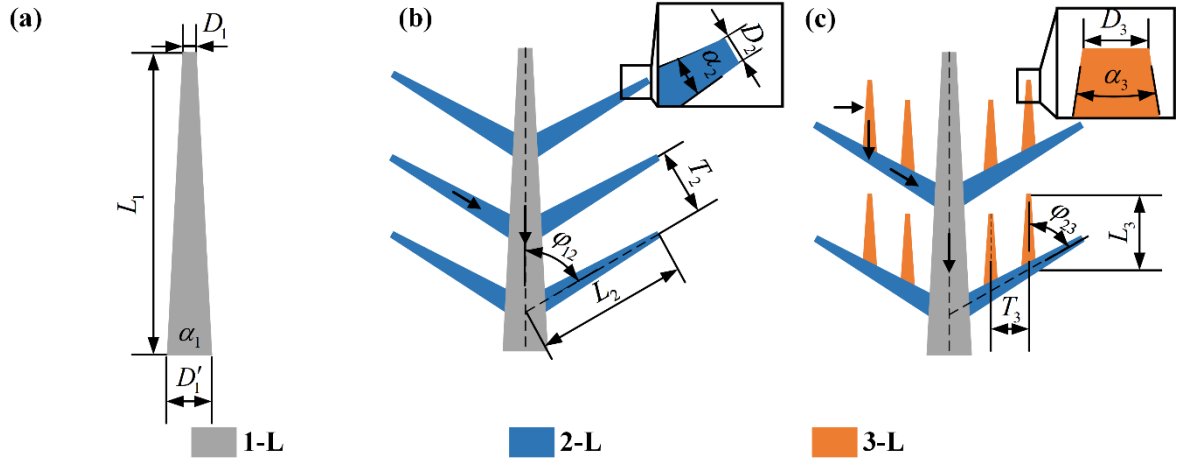


Figure S1. Schematic illustration of the (a) 1Ls, (b) 2Ls, and (c) 3Ls. D_1 and D'_1 are the top and root side of the 1-L corresponding to the central leaf vein. L_1 is the length of the track and α_1 is the wedge angle of the track. D_2 is the top side of the 2-L corresponding to the secondary leaf vein, L_2 is the length of the track and α_2 is the wedge angle of the track. T_2 is the distance of the interval width. ϕ_{12} is the secondary angle between 1-L and 2-L wedge-shaped tracks. D_3 is the top side of the 3-L corresponding to the tertiary leaf vein, L_3 is the length of the track and α_3 is the wedge angle of the track. T_3 is the distance of the interval between the tracks. ϕ_{23} is the secondary angle between 2-L and 3-L.

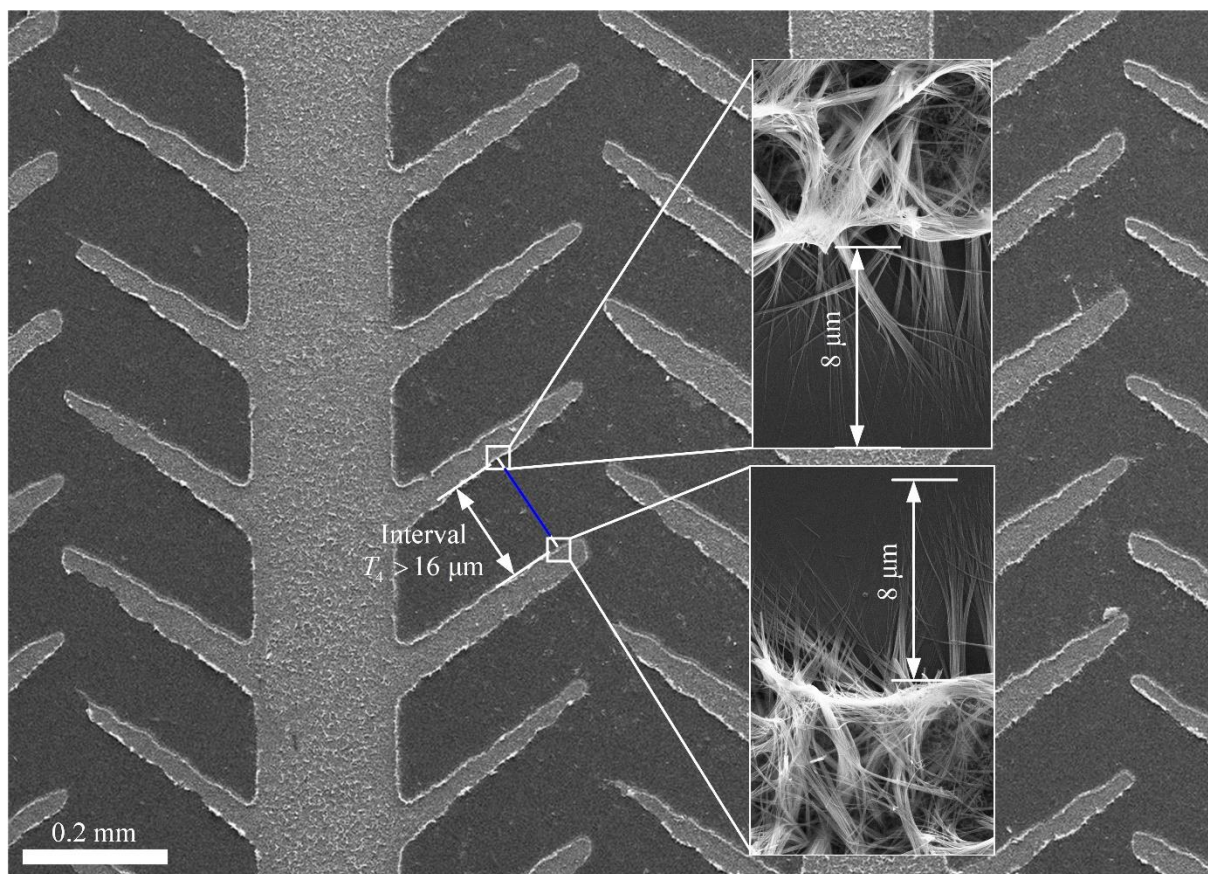


Figure S2. The length of the nanowires on a boundary of the track is about 8 μm . Therefore, the interval width of tracks T_4 should be larger than 16 μm .

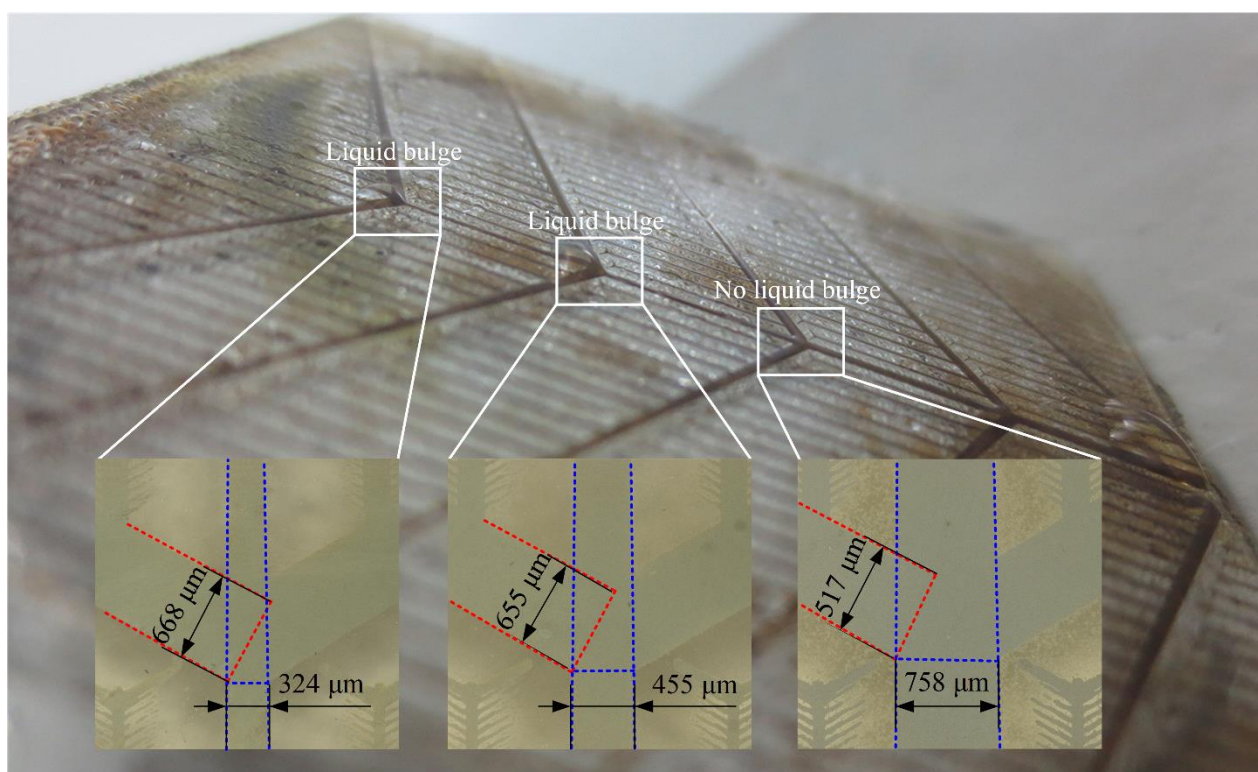


Figure S3. The relationship of the remained droplets vs. the size of the track. If the root side of the higher levels tracks is greater than the width of the lower levels tracks, the water droplet remains on the intersection of tracks. Therefore, the root side of the higher levels tracks should be smaller than the width of the lower levels tracks, avoiding the droplet remains on the tracks in form of a growing bulge.

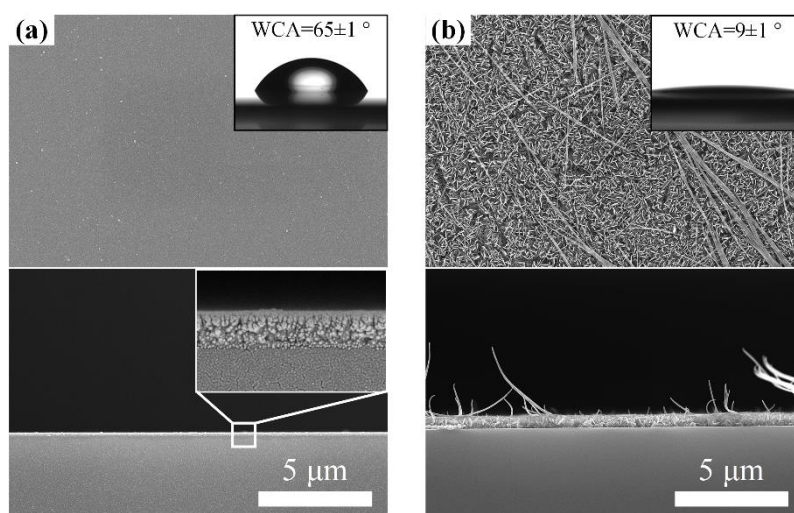


Figure S4. The top and cross-sectional views of microstructures on the substrates immersing in an aqueous solution of NaOH and $(\text{NH}_4)_2\text{S}_2\text{O}_8$ for (a) 0 min, and (b) 30 min. The top-right insets are the WCA measurements of the samples.

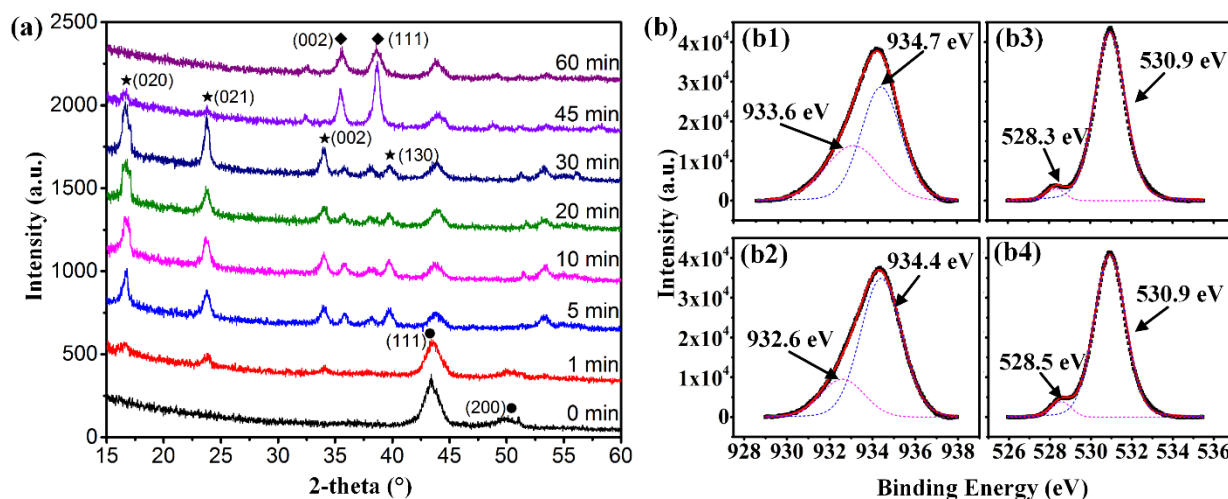


Figure S5. (a) The XRD plot of the samples for different immersion time. The strong peaks marked with circle and observed at $2\theta=43.3^\circ$ and 50.3° are from the pristine Cu nanoparticle layer on the substrate. For an immersion time within 40 min, the peaks marked with star centered at $2\theta=16.7^\circ$, 23.8° , 34° , 39.8° , and 53.4° correspond to (020), (021), (002), (130) and (132) planes of orthorhombic $\text{Cu}(\text{OH})_2$ (JCPDS card No. 80-0076). When the immersion time is prolonged more than 40 min, a high intensity of the peaks observed at $2\theta=35.5^\circ$ and 38.7° correspond to (002) and (111) planes of monoclinic CuO (JCPDS card No. 4-0836), respectively. Thus, we can conclude that the nanowires and nanosheets are composed of $\text{Cu}(\text{OH})_2$ and CuO , respectively. (b) High-resolution XPS spectra of the as-prepared tracks. (b1) and (b2) Core level spectra of Cu 2p for an immersion time of 5 min and 15 min, respectively. (b3) and (b4) Survey spectrums of O 1s Core level correspond to (b1) and (b2). The peaks centered at 934.4 eV and 934.7 eV correspond to Cu 2p $3/2$ electrons of $\text{Cu}(\text{OH})_2$, and the peaks at 932.6 eV and 933.6 eV are related to the Cu 2p $3/2$ signal of CuO (b1 and b2). These results reveal that the peak of $\text{Cu}(\text{OH})_2$ gradually decrease, on the contrary, CuO become a stronger signal with a longer oxidation time. The O 1s spectrum is resolved into two components

centered at 528.5 eV and 530.9 eV that the former peak corresponds to oxygen of CuO and the latter corresponds to oxygen of Cu(OH)₂ (b3 and b4).

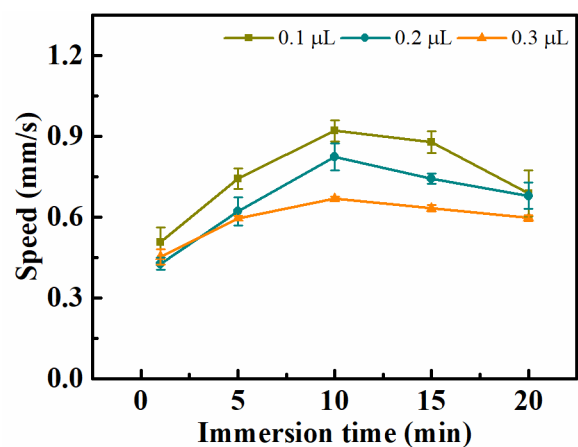


Figure S6. Water spreading speed (v) as a function of immersion time. For a certain volume of water droplet, the water spreading speed increases first and then decrease. The maximum speed is achieved when the immersion time approaches to 10 min.

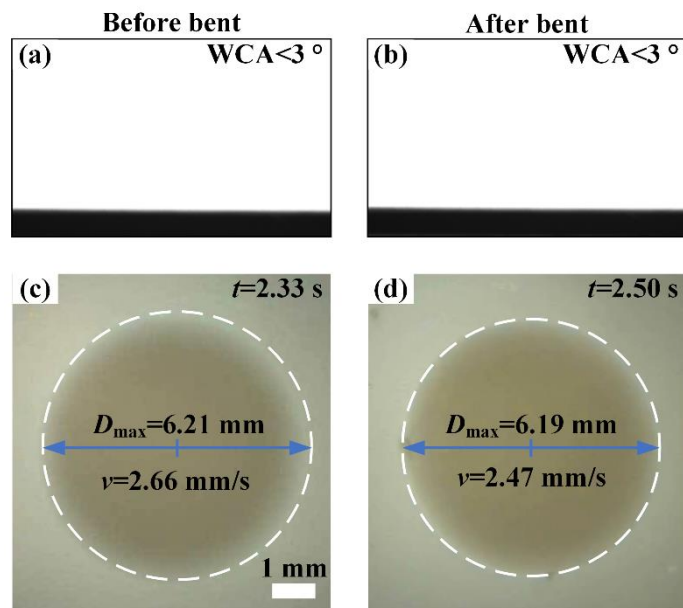


Figure S7. The surfaces with an immersion time of 5 min exhibit superhydrophilicity during the water-spreading test whether being bent (a) or not (b). However, the maximum diameter (D_{\max}) of the water spreading on the surface decreases from 6.21 mm (c) to 6.19 mm (d) and t increases from 2.33 s to 2.50 s, resulting in v decreasing from 2.66 mm s^{-1} to 2.47 mm s^{-1} . From the change of v , the wettability change of the surface before and after being bent can be distinguished.

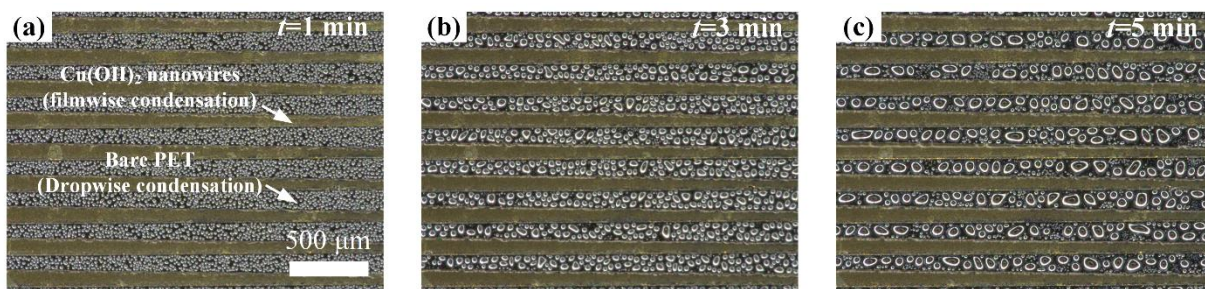


Figure S8. Water condensation on the wedge-shaped tracks. As time goes on, $\text{Cu}(\text{OH})_2$ nanowires tracks exhibit filmwise condensation while dropwise condensation occur on the bare PET regions. (a) 1min; (b) 2 min and (c) 5 min.

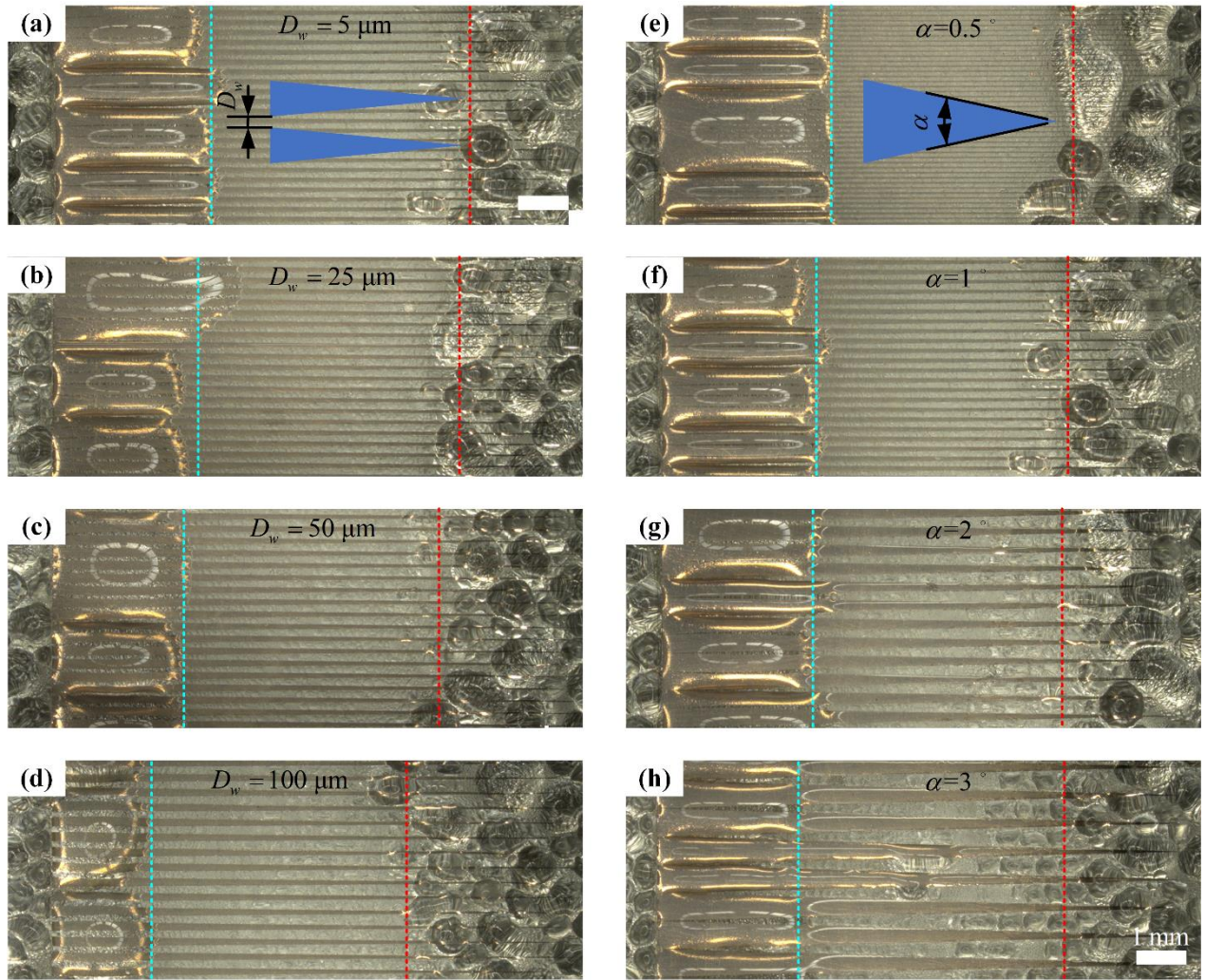


Figure S9. Water collection on tracks with different interval widths (a) 5 μm , (b) 25 μm , (c) 50 μm , and (d) 100 μm . Water collection on tracks with different wedge angles (e) 0.5 $^\circ$, (f) 1 $^\circ$, (g) 2 $^\circ$ and (h) 3 $^\circ$. The region on the left of green hidden lines and the right of red hidden lines presents the water collection region and condensate remained region, respectively.

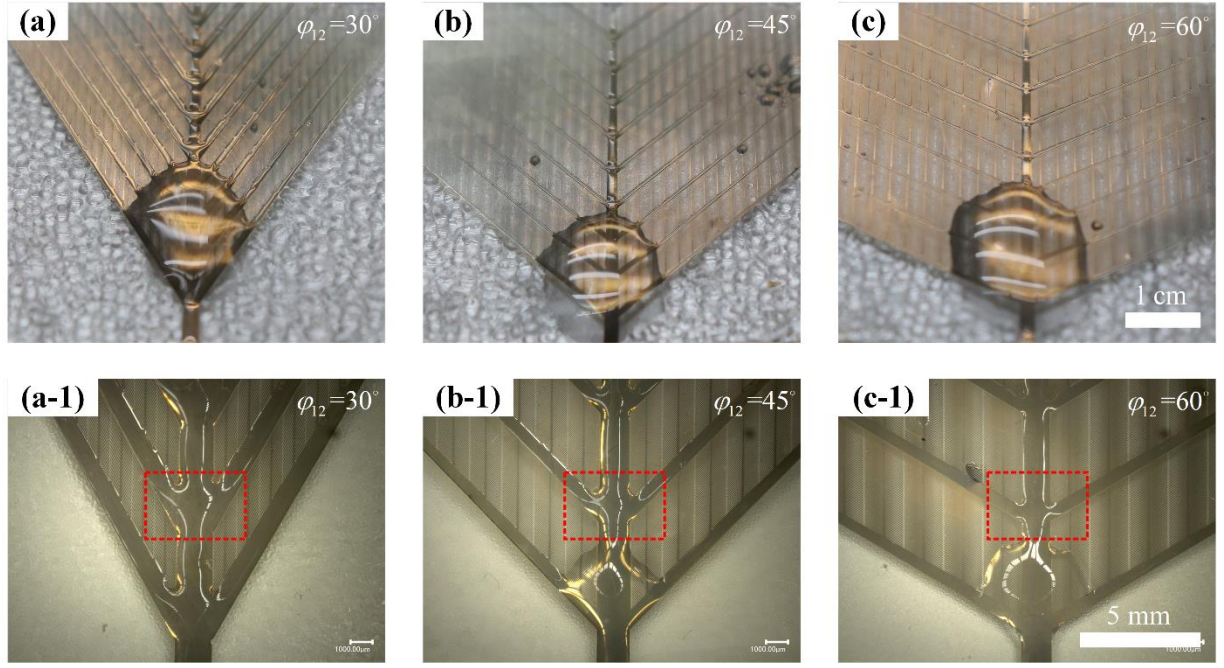


Figure S10. Water collection of the samples with (a) $\varphi_{12}=30^\circ$, (b) $\varphi_{12}=45^\circ$, and (c) $\varphi_{12}=60^\circ$ on the horizontal stage. Image of the water film on the track taken by VHX-1000E, (a-1) $\varphi_{12}=30^\circ$, (b-1) $\varphi_{12}=45^\circ$, and (c-1) $\varphi_{12}=60^\circ$.

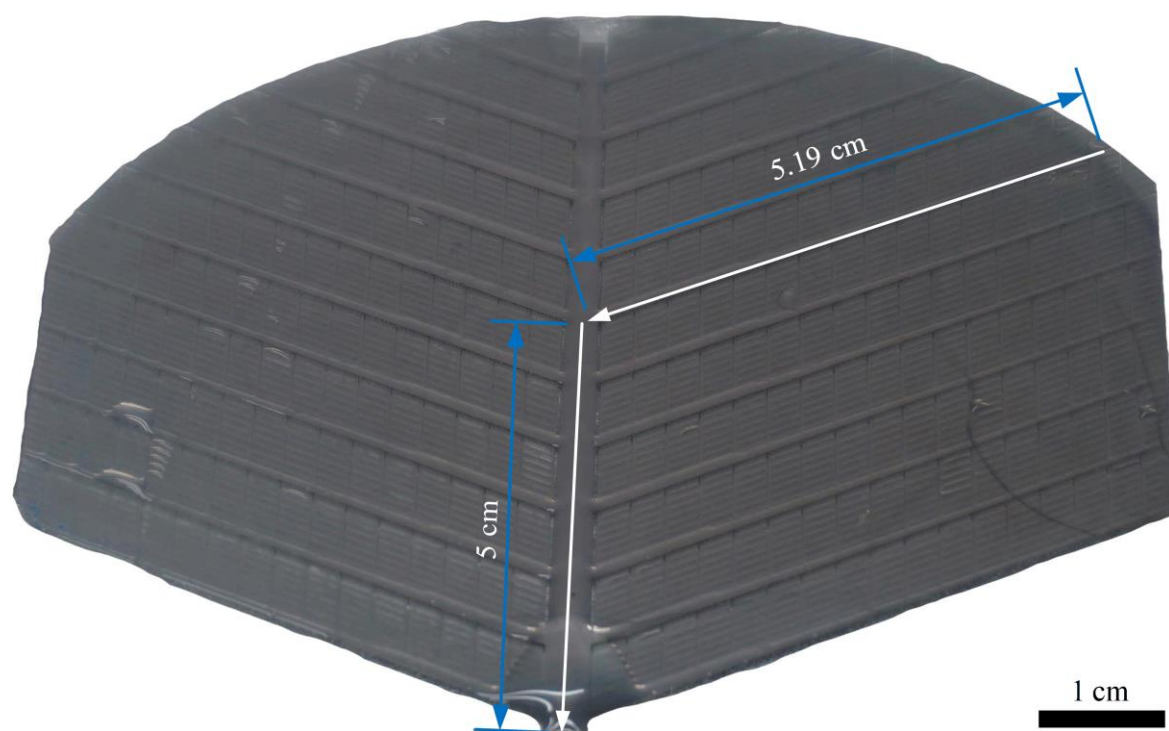


Figure S11. Directional water collection of the five levels wedge-shaped tracks on horizontal plane (10 cm× 10 cm).

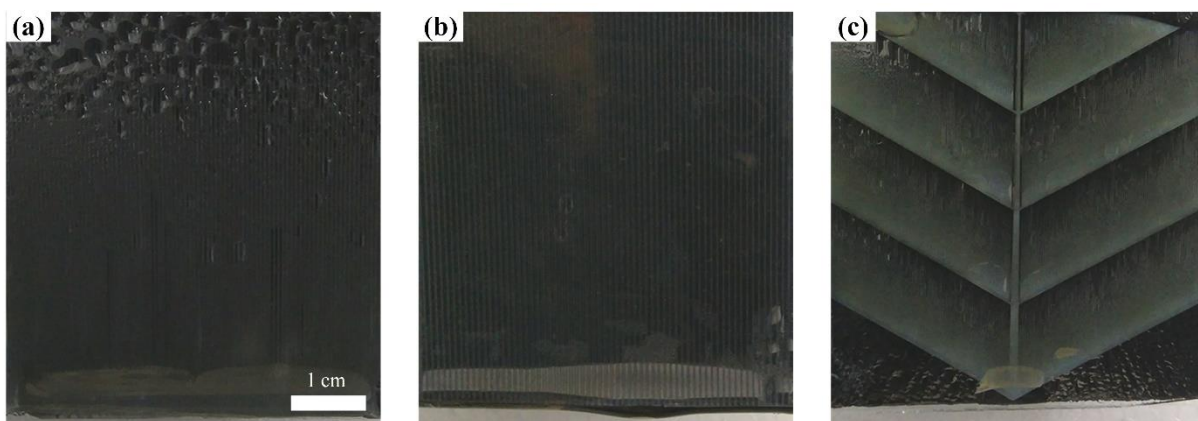


Figure S12. Water collection of (a) 1Ls, (b) 2Ls, and (c) 3Ls on plane surface.

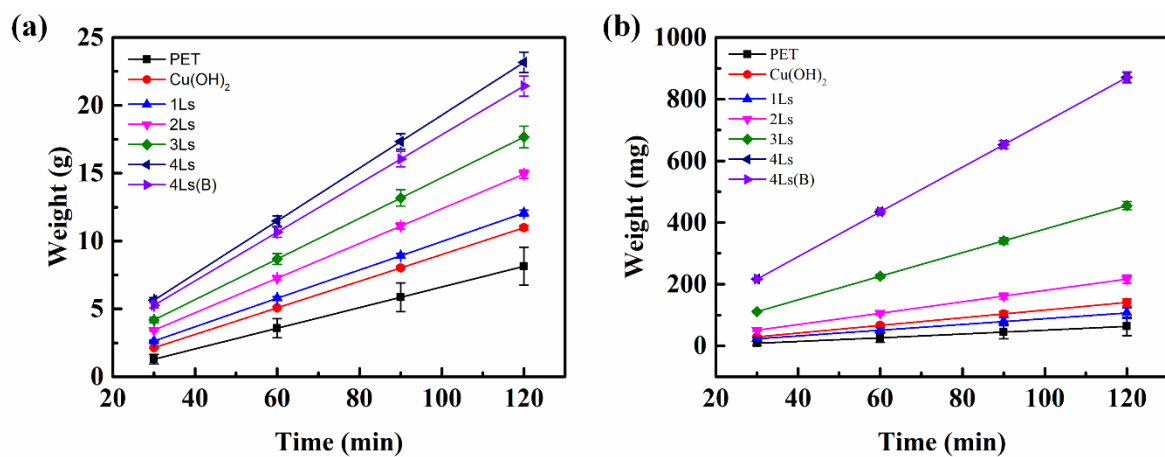


Figure S13. The collected water versus time of different surfaces. (a) Water collection on plane surface. (b) Water collection on cylinder surface.